FINAL TECHNICAL REPORT

(NASA-CR-143086) ION-IMPLANTED EPITAXIALLY GROWN ZnSe Final Report, 1 May 1974 - 30 Apr. 1975 (Colorado Univ.) 49 p HC $3.75
CSCL 20L
N75-26888
Unclas
G3/76 28012

ION-IMPLANTED EPITAXIALLY GROWN ZnSe

NASA Grant No.: NSG-1037

Period Covered by Report: May 1, 1974 to April 30, 1975

Fred Chernow, Principal Investigator
Photoconductive Semiconductors and Devices Laboratory
Department of Electrical Engineering
University of Colorado
Boulder, Colorado 80302

ION IMPLANTED, EPITAXIALLY GROWN ZnSe

Introduction

The use of ZnSe to obtain efficient, short wavelength injection luminescence was investigated. It was originally proposed that shorter wavelength emission and higher efficiency could be achieved by employing a p-i-n diode structure rather than the normal p-n diode structure. The intervening i layer would minimize concentration quenching effects and the donor-acceptor pair states leading to long wavelength emission. The surface p layer would be formed by ion implantation; implantation of the i layer rather than the n substrate would permit higher, uncompensated p-type doping. An ion implanted p-n junction in ZnSe would be expected to be efficiency limited by high electron injection terminating in nonradiative recombination at the front surface and by low hole injection resulting from the inability to obtain high conductivity p-type surface layers. While the injection ratio in pn junctions is fundamentally determined by the ratio of majority carrier concentrations, the injection ratio in p-i-n structures can be determined by the more favorable mobility ratios and/or space charge neutrality requirements in the i layer.

Three basic technical problems must be handled in order to realize this design:

1.) implantation of high resistivity ZnSe to obtain at least moderate p-type conductivity.

2.) epitaxial growth of ZnSe on n-type ZnSe where the epitaxial layer must have both a low concentration of shallow dopants and a low concentration of deep recombination centers.

3.) preparation of single crystal, n-type ZnSe substrates with surfaces suitable for subsequent epitaxial growth.

Conducting, n-type, bulk ZnSe is commercially available. Although this material is advertized as single crystal, it is always severely twinned, and the yield of single crystal wafers of sufficient area would be very low. Polishing and etching ZnSe for epitaxial growth is also difficult. The close spaced transport process was chosen for growth of the intrinsic layer. Since this process would be developed and since epitaxial growth of ZnSe on Ge and GaAs is known to yield good quality ZnSe layers, epitaxial growth by the same process was chosen for preparing the n-type base layer. The chemical, close spaced transport process was selected to yield thick enough layers to permit low resistance, lateral electron flow.

The problem was approached in its separate parts. During the first year of this program the growth of undoped ZnSe epitaxial layers on Ge substrates and a study of their luminescent properties was completed. This work was reviewed in the first year report and reported in the accompanying preprint. Growth of doped ZnSe layers on Ge and GaAs substrates, annealing to obtain n-type conductivity, and the photoluninescent and electroluminescent layers was studied in the second year. Implantation of intrinsic layers and growth of intrinsic layers on doped layers was initiated in the second year. The text of this report concerns the findings of the second year's work and the conclusions for the project as a whole.

ZnSe-HCl growths

Approximately 50 ZnSe layers were grown on Ge or GaAs substrates by the chemical vapor transport technique using H_2 + HCl.(1,2) The growth system and the method of preparing Ge substrates are described in the enclosed preprint. GaAs substrates were prepared from p-type (100) wafers using the etch described in detail below.(3)

1.) one part distilled H_2O
2.) add five parts H_2SO_4
3.) cool partially in water bath
4.) add one part 30% H_2O_2
5.) cool to room temperature
6.) etch for 30 minutes

A "random" motion of the crystal during step (6) is required to obtain uniform etching; simple stirring of the solution leads to preferential etching along flow lines.

The growth procedure for ZnSe-H_2-HCl growths was basically the same as that described previously for ZnSe-H_2 growths; i.e.,

1.) flush growth tube with Pd-Ag purified H_2 for a minimum of one hour.
2.) set H_2 flow to value established for growth, set source and substrate controls for 350°C, and bake out growth region for at least one hour.
3.) set substrate control for 575°C and source control for 675°C, set HCl flow to obtain desired HCl percentage in the flow gas.
4.) allow ZnSe growth to proceed for a time period of two to twelve hours.
5.) stop HCl flow, cut power to source and substrate heaters, and substitute flow of Ar purge gas for H_2 flow.

The Ar flow at step (5) slows the rate of substrate cooling, but the bulk of the cool down to room temperature occurs in less than 15 minutes. Programmed, slow cool downs to room temperature were not used. Although this capability was provided, the necessity of quench cooling after subsequent annealing made this capability irrelevant. All the as-grown ZnSe-HCl layers exhibited high resistivity.

ZnSe - 0.02%HCl - Ge

These growths lead to epitaxial ZnSe layers showing extreme, macroscopic variations in thickness to the point that there may be incomplete substrate coverage in some regions of the sample. The growth rate implied by the thickest regions of these layers is no greater than would be obtained in the absence of HCl. The morphography in these thick regions is identical to that observed in the absence of HCl.

Figure 1 shows a typical UV stimulated fluorescence spectrum taken at a sample temperature of 77°K. This spectra is unique to this HCl concentration. A similar line has been associated with Cu in ZnSe.(4) The second line at ∿6400Å that has been associated with a second valence state of Cu does not appear in these samples.

HCl in concentrations of 0.02% does not lead to a sufficient growth rate or layer uniformity to be useful in producing doped ZnSe base layers.

ZnSe - 0.6%HCl - Ge

This HCl concentration yields a ZnSe growth rate of 31 microns/-hour and good macroscopic uniformity. Laue X-ray measurements show

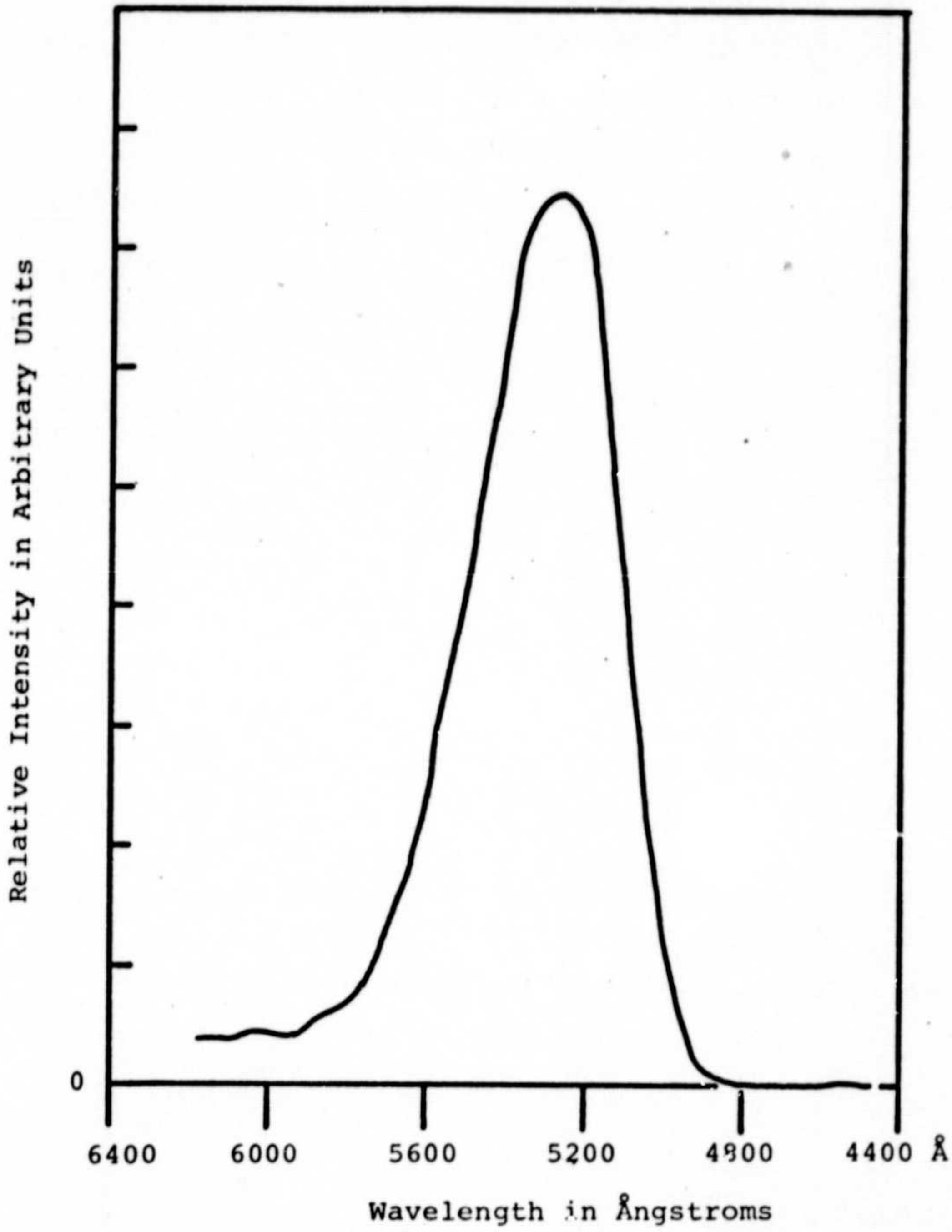

Figure 1

UV Stimulated Fluorescence Spectra of a
ZnSe-0.02% HCl Epitaxial Layer at 77°K

polycrystalline ring patterns. The morphography shows the irregularities typical of polycrystalline layers; typical lateral dimensions of the crystallites lie in the range of 30-50 microns. There is no evidence of thermal-stress induced cracking in layers as thick as 200µ.

The UV stimulated fluorescence at 77°K is a uniform, bright orange. The spectra and intensity in the neighborhood of this ∿6000Å line is virtually identical to that obtained from samples grown in 0.2% HCl (see Fig. 3). There is no emission at wavelengths below 5000Å however.

The polycrystalline nature of these layers makes them unsuitable for subsequent ZnSe epitaxy.

ZnSe - 0.2%HCl - Ge

This HCl concentration leads to the most satisfactory, thick, epitaxial ZnSe layers on Ge. The growth rate is 5 microns/hour. Macroscopic uniformity of the layer thickness across the sample is ±10%. Occasionally these layers exhibit a few cracks associated with stressing during cool down. Figure 2a is a phase contrast photograph showing typical surface morphography; the field of view in this figure is approximately 15x20 microns. These layers are a clear lemon-yellow; it is readily possible to focus on the Ge surface through the ZnSe using a microscope.

Figure 3 shows a typical UV stimulated fluorescence spectra at 77°K. The line at 6000Å agrees in center wavelength and linewidth with the donor acceptor pair line observed in bulk ZnSe after correction for photocathode response and spectral slit width.$^{(5)}$ The line between 4560Å and 4720Å is the remnants of the phonon assisted series observed in ZnSe layers grown in pure H_2.$^{(6)}$ The line at 4460Å is the 4454Å bound exciton line broadened and shifted to longer wavelength.

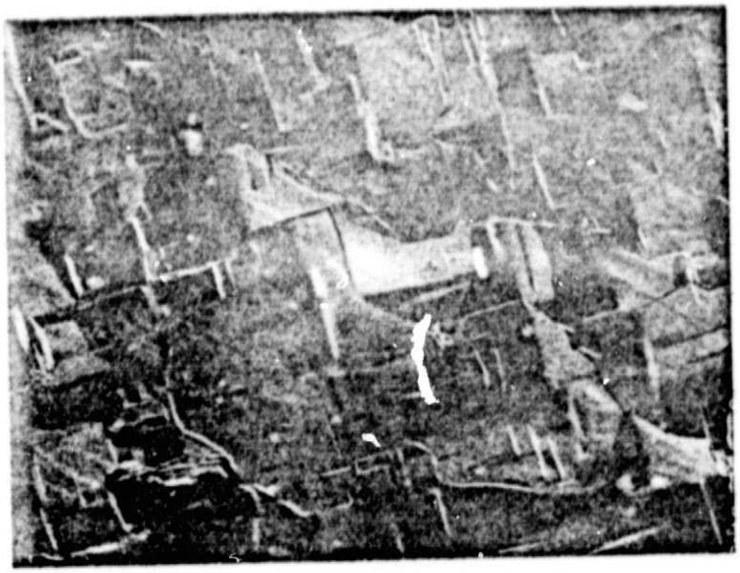

Figure 2a

Morphography of Epitaxial ZnSe on (100) Ge

HCl concentration = 0.2%

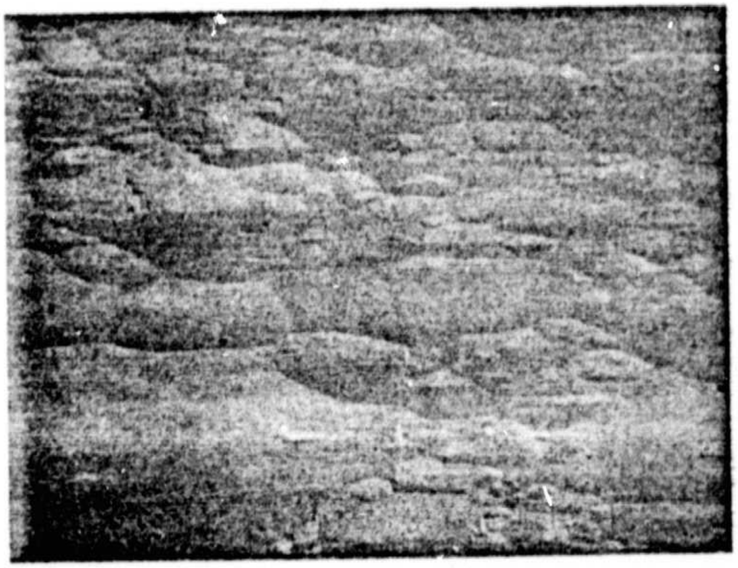

Figure 2b

Morphography of Epitaxial ZnSe on (100) GaAs

HCl concentration = 0.6%

ZnSe - 0.1%HCl - Ge

ZnSe layers grown at this HCl concentration show characteristics of both .02% and .2% HCl concentrations. The central region of the growth area exhibits the morphography of 0.2% HCl growths and a growth rate of two microns/hour. The outer region shows the morphography and growth rate of the lower concentration. There is an abrupt and irregular transition between these two zones.

The UV stimulated fluorescence spectra at 77°K is included in Figure 3. Relative to the 0.2% HCl growths the orange intensity is reduced, the short wavelength intensity is increased, and the shift and broadening of the bound exciton line is reduced.

Irregularity in the morphography and growth rate makes these layers unsuitable for subsequent ZnSe epitaxy.

ZnSe - 0.6%HCl - GaAs

At this HCl concentration, epitaxial ZnSe layers grown on GaAs substrates at an average rate of 1.5 microns/hour. Macroscopic thickness uniformity across the surface of the sample is ±20%. Figure 2b is a phase contrast photograph showing typical morphography of these samples; the field of view in this figure is approximately 15 by 20 microns. Faceting in these samples is relatively minor compared to 0.2% HCl layers grown on Ge. There is a tendency for a few, very high (5-10 micron) pyramidal growth features to appear in each sample. The UV stimulated fluorescence spectra of these samples at 77°K is comparable to that of 0.6% HCl layers grown on Ge; i.e., an intense emission band at ∿6000Å and no emission at wavelengths below 5000Å.

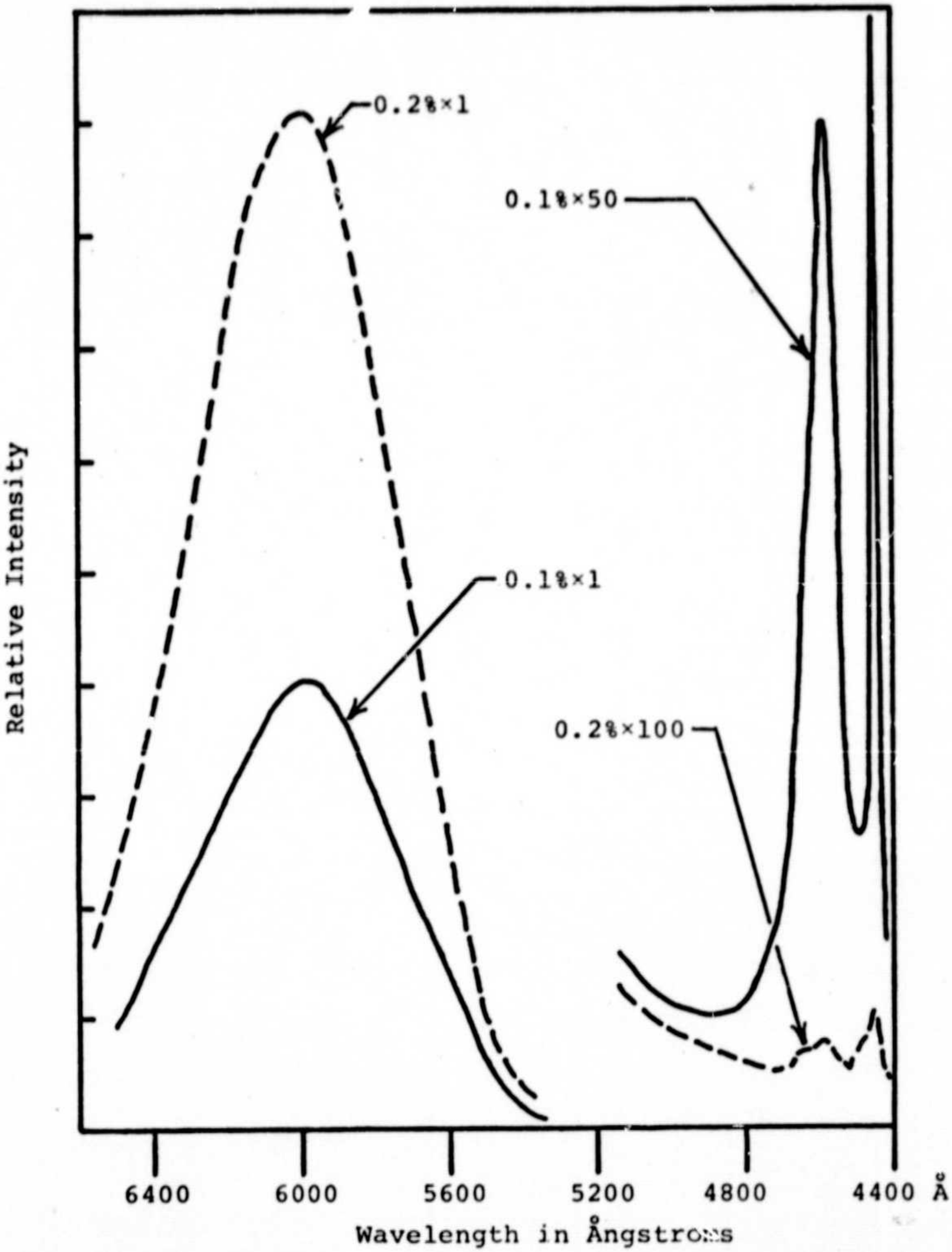

Figure 3

Comparison of UV Stimulated Fluorescence Spectra of ZnSe-0.2% HCl and ZnSe-0.1% HCl Layers at 77°K

Reduction of the HCl concentration below 0.6% leads to very low growth rates, macroscopic thickness non-uniformity, and erratic morphography. The requirement for higher HCl concentrations when using GaAs substrates is probably a reflection of the action of Ge as a transport agent in the ZnSe-HCl-Ge case. Higher incorporated Cl concentrations are anticipated in acceptable ZnSe layers on GaAs and counter doping effects are expected to be more severe.(7)

Zn Annealing and Conductivity

A number of ZnSe layers on Ge were annealed in Zn vapor. High purity Zn pellets were sealed in evacuated quartz ampoules along with the sample. The ampoule was necked down at the center to insure separation of the solid or liquid Zn and the sample during annealing. In the first series of experiments, the ampoules were inserted into a preheated, single temperature zone furnace. The samples were annealed for times between one and sixty hours and the ampoules were quench cooled in water at the end of that time. All of these anneals were performed at 575°C; this equals the substrate temperature during growth. In cases where the quantity of included Zinc greatly exceeded that quantity necessary to establish the $Zn_{(l)} \leftrightarrow Zn_{(g)}$ equilibrium, the Ge substrate appeared to have melted during the anneal. This must have occurred via Zn vapor attack of the substrate to form a Zn-Ge alloy.(8) Reducing the quantity of included Zn to the approximate minimum required to establish the $Zn_{(l)} \leftrightarrow Zn_{(g)}$ eliminated the problem of destroying the substrate, but the conductivity and photoluminescence properties of the resulting ZnSe layers were not reproducible. There was also a consistent loss of photoluminescence efficiency proportional to the n-type conductivity induced. There was no evidence of cracking or peeling of the ZnSe layers except in cases where the substrate was severely attacked. There was always some evidence that the Ge had been attacked, but this was not reproducible either. The reproducibility problem was associated with problems in determining and measuring the quantity of Zinc required. The annealing furnace was converted to a two temperature zone configuration to eliminate this problem. Ampoules for annealing were prepared as before except that the end of the ampoule containing the Zinc pellet was located in the controlled, low temperature zone. This configuration permits independent control of the annealing temperature and the Zinc vapor pressure over the sample. The Zn pellet temperature must be lower than the sample temperature to prevent Zn condensation on the sample. Assuming that the Zn pressure over the sample is proportional to the Zn pressure over the Zn source and the Zn vacancy concentration is controlled by a chemical equation of the form

$$Zn + V_{Zn}^{-p} = pe$$

implies a relationship between the Zn pressure (P_{Zn}) and the electron concentration (n) of the form

$$P_{Zn} = \frac{n^p}{N_D - n} K(T)$$

where N_D is the donor concentration and K(T) is the reaction constant. This relationship was examined for ZnSe layers grown in HCl. The Chlorine concentration in these samples exceeds 10ppm in all probability.(1,9) This corresponds to a donor concentration exceeding $5 \times 10^{17}/cm^3$ and a maximum conductivity of $\sim 10 (\Omega\text{-cm})^{-1}$ if compensation were negligible. Figure 4 shows the sheet conductivity as determined by a four-point probe as function of the equilibrium Zn pressure over the Zn source. The sample temperature was set at 575°C in all cases. These data are reproducible and attack of the Ge substrate is superficial or absent in all cases. Both of the samples shown in Figure 4 were approximately 35 microns thick. No dependence of conductivity on annealing time was found, and it appears that equilibrium is established in a time less than the shortest annealing time of 8 hours.

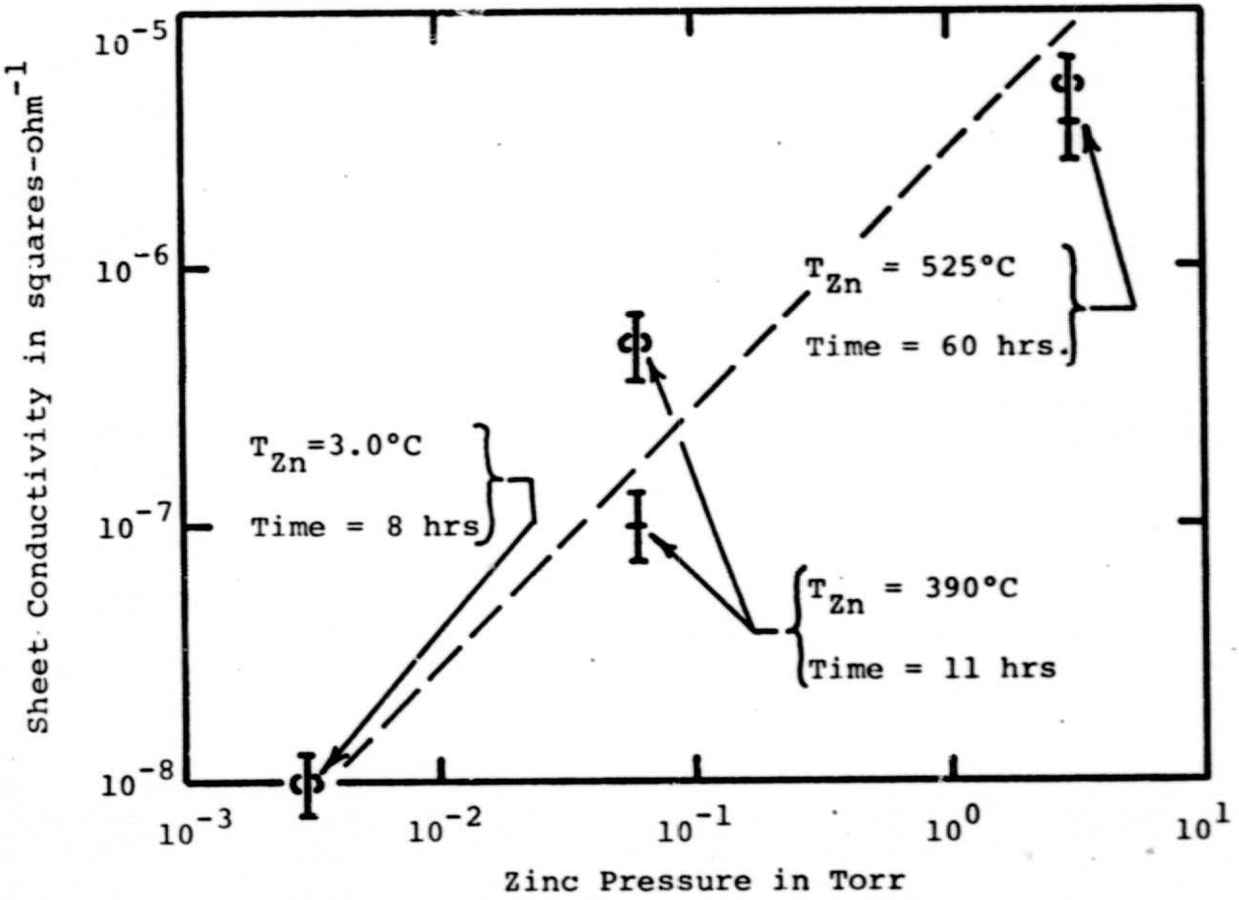

Figure 4

Sheet Conductivity as a Function
of Zn Pressure during Annealing

Assuming that a macroscopic diffusion process is involved, this would require a diffusion constant in excess of $10^{-9}cm^2/sec$ at 575°C. This value may not be unreasonable for Zn vacancies. The magnitude at the induced conductivity is very disappointing. The highest conductivity measured of $\sigma t = 5x10^{-6}/ohm^{-1}$ implies $\sigma \sim 10^{-3}ohm^{-1}cm^{-1}$ assuming a 36 micron layer of uniform conductivity. This implies that less than one donor in 10^4 leads to a free electron; the remainder are either unionized or remain compensated. If it is assumed that the linear relationship between G and P_{Zn} can be extrapolated and that inadequate P_{Zn} was the cause of low conductivity, the Zn temperature would have to be raised to ∿700°C to obtain a σt value of $10^{-3}ohm^{-1}cm^{-1}$ layer. This is the approximate value required to obtain a low series resistance LED assuming that electrons are supplied by lateral flow. This temperature increase would require an increase in the sample temperature and the effect of this on K(T) is not known.

The hypothesis of uniform doping was examined by performing four-point probe conductivity measurements after etching off a fraction of the ZnSe layer. This series of experiments revealed still more serious problems. Initially, the layers were etched back a few microns using a $K_2Cr_2O_7+H_2SO_4$ solution at 50°C. This procedure revealed a few major cracks in all samples. These cracks could not be detected in annealed, unetched samples, but preferential etching makes them readily visible. A second collection of samples were etched back using a Br-Methanol solution on the remote chance that the ionic etch promoted crack propagation. The same crack pattern was revealed by the Br-Methanol etch.

A series of etching experiments was performed to determine the origin of these cracks. Etching as-grown ZnSe layers did not reveal any hidden cracks; this eliminates the possibility that cracks form during the relatively rapid cool down (∿15 minutes) from the growth temperature. Samples were then cooled down after annealing in Zn in times comparable to the cool down time after growth. Although etching did not reveal any cracking in these samples, electrical measurements indicated negligible induced conductivity. Finally, one sample was slow cooled to approximately 300°C and then quenched to room temperature. The sample and the Zn source were both brought to 300°C in this intermediate step from 575°C and 525°C, respectively. The conductivity of the layer was identical to that obtained from samples quench cooled from T_{sample}=575°C and T_{Zinc}=300°C. Etching did not reveal any cracks however. It can be concluded that compensation is a very fast process in ZnSe and that balancing thermal stress problems against compensation problems may be very difficult. Incorporation of shallower group III donors such as Ga or Al by doping the source crystals might be advisable.(10)

In general, this cracking problem is not severe; the density of cracks is only about four per centimeter and large useable areas remain available. The conductivity of a few samples was measured using the four point probe and sequential etching. The data indicate that the induced conductivity is not uniform; the conductivity per unit thickness is much higher near the ZnSe surface exposed to the Zn atmosphere. This result does not appear at first to be consistent with the results implying rapid equilibration. Four point probe measurements were then performed on the Ge substrate after the annealed ZnSe layer had been completely removed. The apparent conductivity of the Ge is measurably higher than that of unused Ge substrates. Thermal probe measurements indicate a definite p-type signal while these measurements on unused substrates are inconclusive. It is probable that the Ge substrate is acting as a sink for Zn. Data for Zn diffusion in Ge at 585°C indicate that Zn should not diffuse more than 500Å during growth and annealing.(11) The change in conductivity of the Ge and an assumed diffusion depth of 500Å implies that the Ge is doped degenerately with Zn acceptors to this depth. It is possible that during annealing that Zn vacancies are generated continuously at the ZnSe-Ge interface. These vacancies would diffuse through the ZnSe and be annihilated at the exposed surface. This model leads to a steady state situation where the induced conductivity varies with depth. This model also suggests that the n-type conductivity that can be achieved in ZnSe epitaxial layers may be severely limited.(12)

Heterojunction I-V Characteristics

I-V characteristics of the ZnSe-Ge heterojunction originally were of no interest to this study. The Ge substrates were chosen to be undoped in order to avoid unnecessary contamination of the epitaxial ZnSe layers. Since the electron affinities of ZnSe and Ge do not lead to an interface spike in the conduction band edge, the electrical characteristics of this heterojunction have been studied extensively, however.(13,14) The relatively high resistivity ZnSe-HCl obtained after annealing in Zn and the undoped Ge substrate should not lead to a readily observable p-n junction. This occurs because the Fermi levels should be approximately 0.35eV below the conduction band in both materials. Since there is no diffusion potential at the interface, the forward I-V characteristics should be dominated by series resistance. If, on the other hand, the Ge substrate is heavily doped p-type by diffused Zn, a p-n junction should be observed in the I-V characteristics.

Contacts were applied to a number of Zn annealed samples in order to test this hypothesis. In or In-Sn contacts were soldered on the Ge substrates. In or Al contacts were vacuum deposted on the ZnSe to provide electron injecting contacts to the ZnSe. Au contacts were vacuum deposited on the ZnSe in cases where electron rectifying contacts to the ZnSe were desired. It was found that a glow discharge in H_2 prior to deposition was essential in order to obtain good contact adhesion. Electrical leads to the ZnSe contacts were established using Au-wire springs, and leads to the Ge were made by soldering wires to the In or In-Sn pads.

I-V characteristics were taken using conventional D.C. techniques. Results were recorded on an x-y plotter and an electrometer interface was provided between the sample and the plotter.

Electron injection contacts on the ZnSe should lead to familiar diode characteristics if the Ge is doped p-type. Negative potential applied to the ZnSe should correspond to forward bias. In contrast to expectation, the "forward" and "reverse" characteristics of the junction were virtually identical. The current was superlinear in voltage and the linear region near the origin did not exceed 1 volt.

An estimate of the diffusion potential obviously cannot be obtained from this data. In fact, the Ge appears to be acting as an electron injecting contact to the ZnSe. Electron injection appears to be impossible due to both the thermal probe data and published electron affinity data. The characteristics do show evidence of space charge limited current, however. Reducing the sample temperature to 77°K did not alter the symmetry of the characteristics or their SCLC-like nature. Light emission was not observed at 77°K or 300°K in either polarity.

A model explaining these results was obtained from samples having electron rectifying contacts on the ZnSe.

Au on n-type, conducting ZnSe, yields a 1.36eV electron barrier.(15) The depth of the Fermi level (0.35eV) for ZnSe-HCl samples annealed in Zn suggest that the electron barrier would be $\sim$1.0eV in this case. Since the behavior of this contact is well-known, the nature of the ZnSe-Ge contact can be investigated.

Figure 5 shows the room temperature, heterojunction I-V characteristics of sample #74. Sample #74 is the layer that was annealed in a high Zn pressure, slow cooled to an intermediate Zn pressure, and finally quench cooled to room temperature. Four terminal surface measurements indicated a resistivity typical of a low Zn pressure anneal. In contrast to normal procedure, contact to the ZnSe on #74 was made with a gold plated spring lead rather than a deposited Au film. Prior to the heterojunction measurements, the sample was etched for 2 minutes in 0.1% Br-Methanol to remove approximately 5 microns from the surface of the 35 micron thick sample. The sheet resistivity was too high to measure after etching.

The data shown in Figure 5 are typical of SCLC with trap filling. The reverse characteristic ($ZnSe^{(-)}$-$Ge^{(+)}$) is linear with a resistance of $2.5 \times 10^9 \Omega$; there is no evidence of a saturation of the Au-ZnSe contact at low voltages. The forward current ($ZnSe^{(+)}$-$Ge^{(-)}$) is quadratic in voltage at high forward bias; this is shown in the overlay of discrete points which are proportional to the square root of the current at each voltage. The rapid rise in current at 1.3-1.5 volts can be explained by at least three mechanisms. This threshold voltage is sufficient to eliminate the Au-ZnSe contact barrier if all the applied voltage appears here. Hole injection into the ZnSe could occur at this point, but the SCLC characteristic at higher voltage would be difficult to explain. This threshold could be a simple trap filling process, but this requires that the Ge act as an electron injecting contact to the ZnSe. Since the Ge is p-type, it cannot act as a simple electron injecting contact. Ge can act as an electron injecting contact to ZnSe if one postulates that these electrons are injected into the ZnSe conduction band by tunneling from the Ge valence band. The 1.3-1.5 threshold is believed to be associated with this tunneling process. Figure 6 shows the heterojunction characteristics for a ZnSe grown in H_2 only. The layer was annealed in Zn and then etched

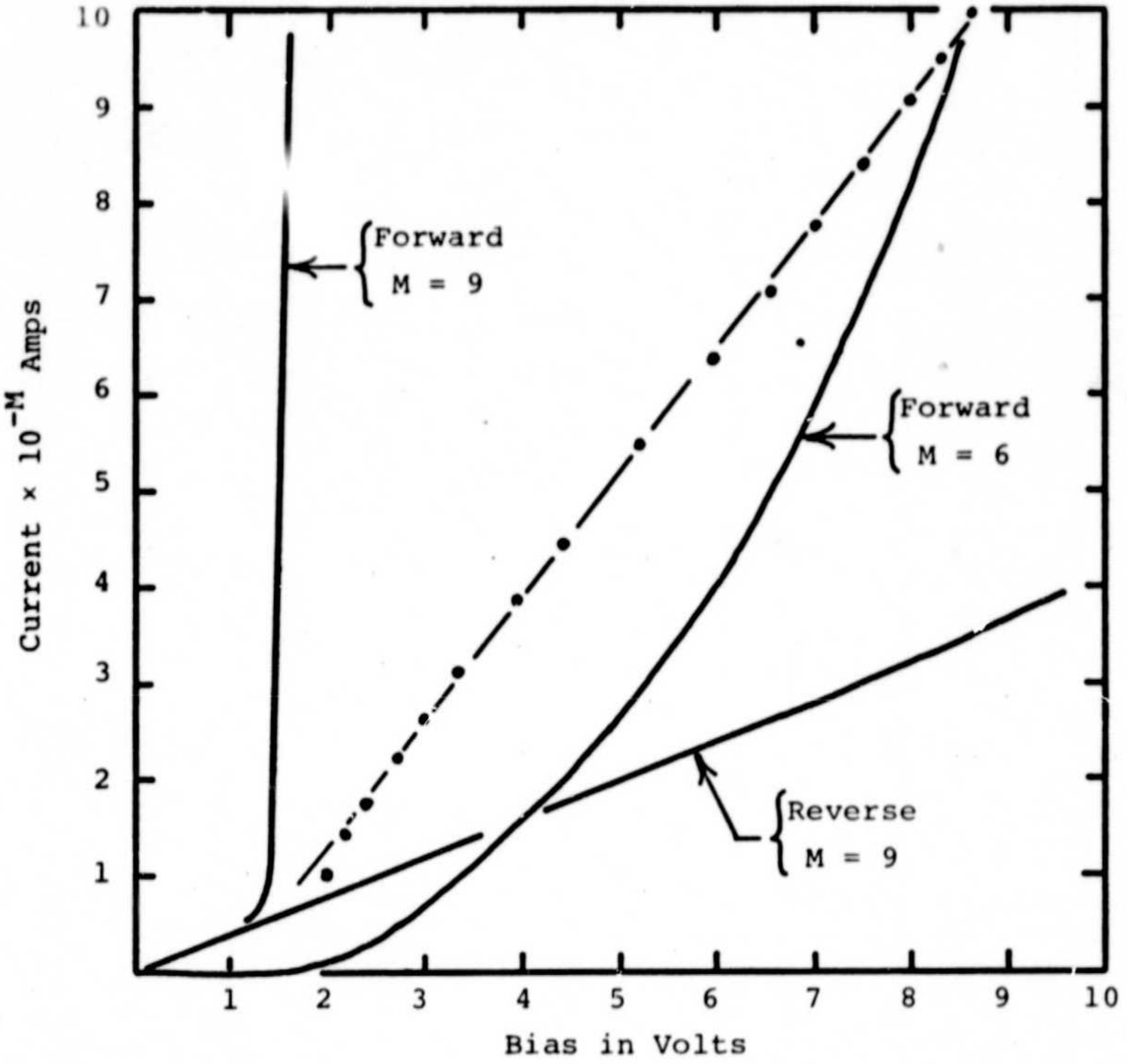

Figure 5

I-V Characteristic
ZnSe(+)-Ge(-) corresponds to forward bias. Discrete points are the square root of the forward characteristic on an arbitrary scale.

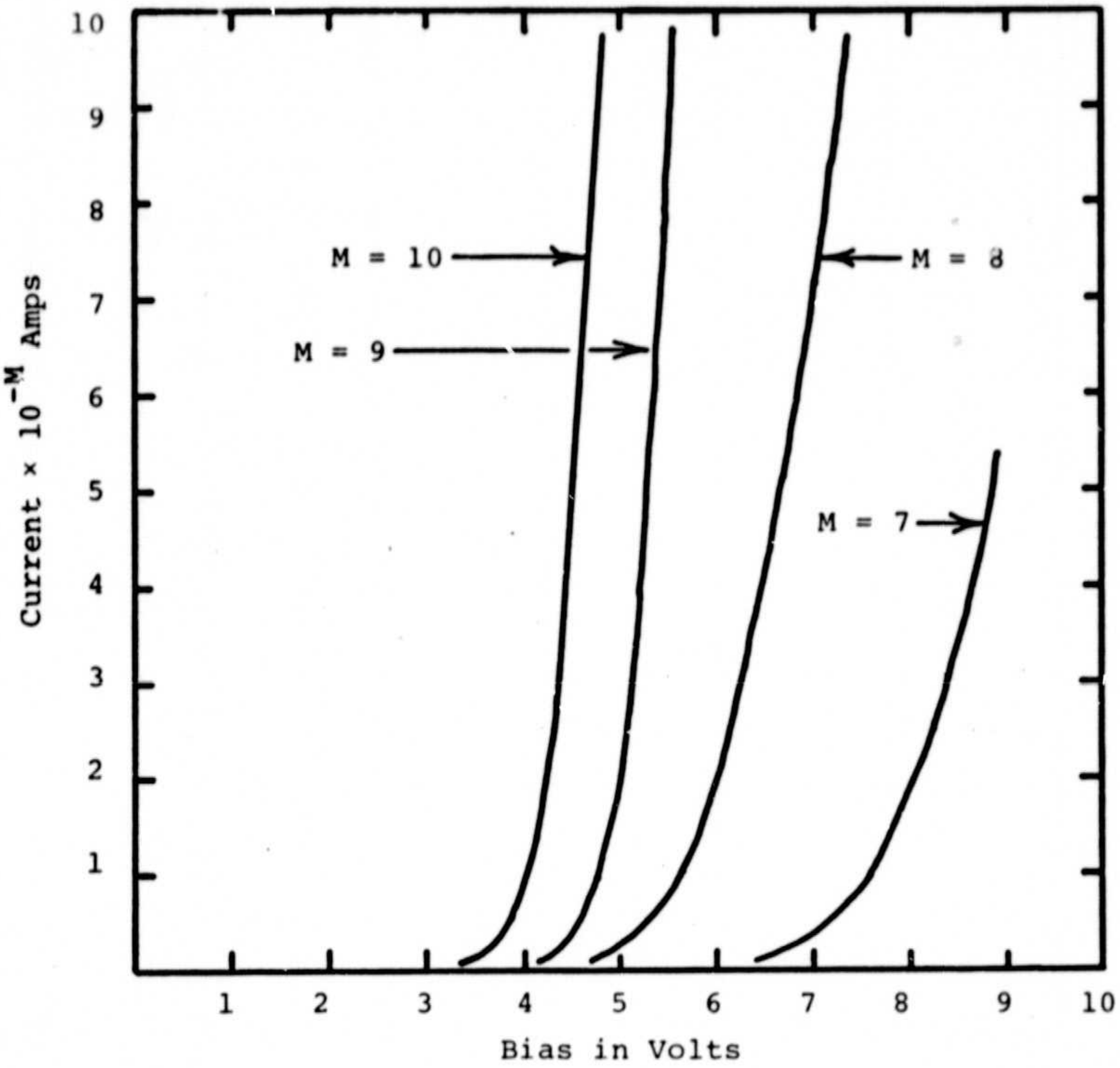

Figure 6

Forward I-V Characteristic for a
Zn annealed but undoped ZnSe layer.

to leave less than a two micron ZnSe layer. Contact to the ZnSe was made with a gold plated spring wire. The reverse current $Au^{(-)}-Ge^{(+)}$ was less than 10^{-11}A at 10 Volts. The forward current $Au^{(+)}-Ge^{(-)}$ could not be plotted continuously using more sensitive current scales and the threshold for superlinear behavior was not determined. The forward current increases as the tenth or higher power of the voltage throughout the measurable range. Attempts to observe SCLC in the trap filled limit led instead to permanent breakdown at approximately 16 Volts.

Figure 7 shows the heterojunction characteristics of a second ZnSe-HCl layer at room temperature; this sample was annealed so as to yield the highest ZnSe conductivity (see Figure 3). The area of the Au contact on the ZnSe was $2x10^{-3}cm^2$. Several indium contacts were soldered to the front surface of the Ge substrate to reduce series resistance. The reverse characteristic ($ZnS^{(-)}-Ge^{(+)}$) is linear with a resistance of $1.4x10^6\Omega$ throughout the measurable range. The breakover to a second linear range is believed to be due to tunneling from the Ge valence band to the ZnSe conduction band. The second linear range is believed to be due to the bulk series resistance of the ZnSe. The differential resistance of $8x10^4\Omega$ in this range implies a resistivity of approximately $5x10^4\Omega$-cm for the ZnSe; this is in good agreement with the data from four point probe measurements performed on the surface. The superlinear behavior beginning at approximately 2 Volts is approximately quadratic. Experiments performed with varying numbers of the Ge contacts connected suggest that the deviation from quadratic behavior are due to series resistance in the Ge.

Figure 8 shows the forward I-V characteristics of the same sample at liquid nitrogen temperature. The initial resistance and

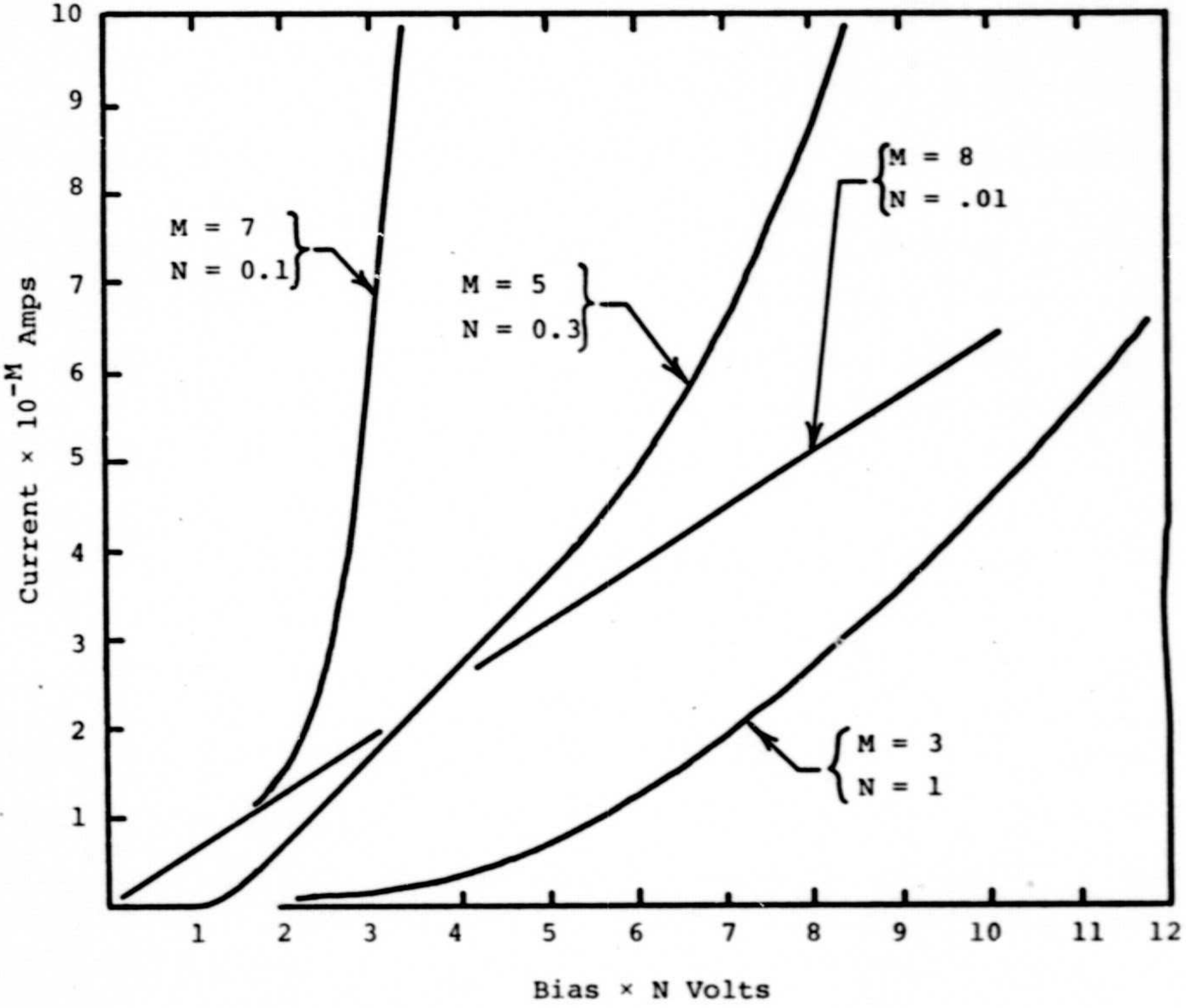

Figure 7

Forward I-V Characteristic at 300°K of an 0.2% HCl ZnSe Layer annealed in Zn pressure of 3 Torr (see Figure 3).

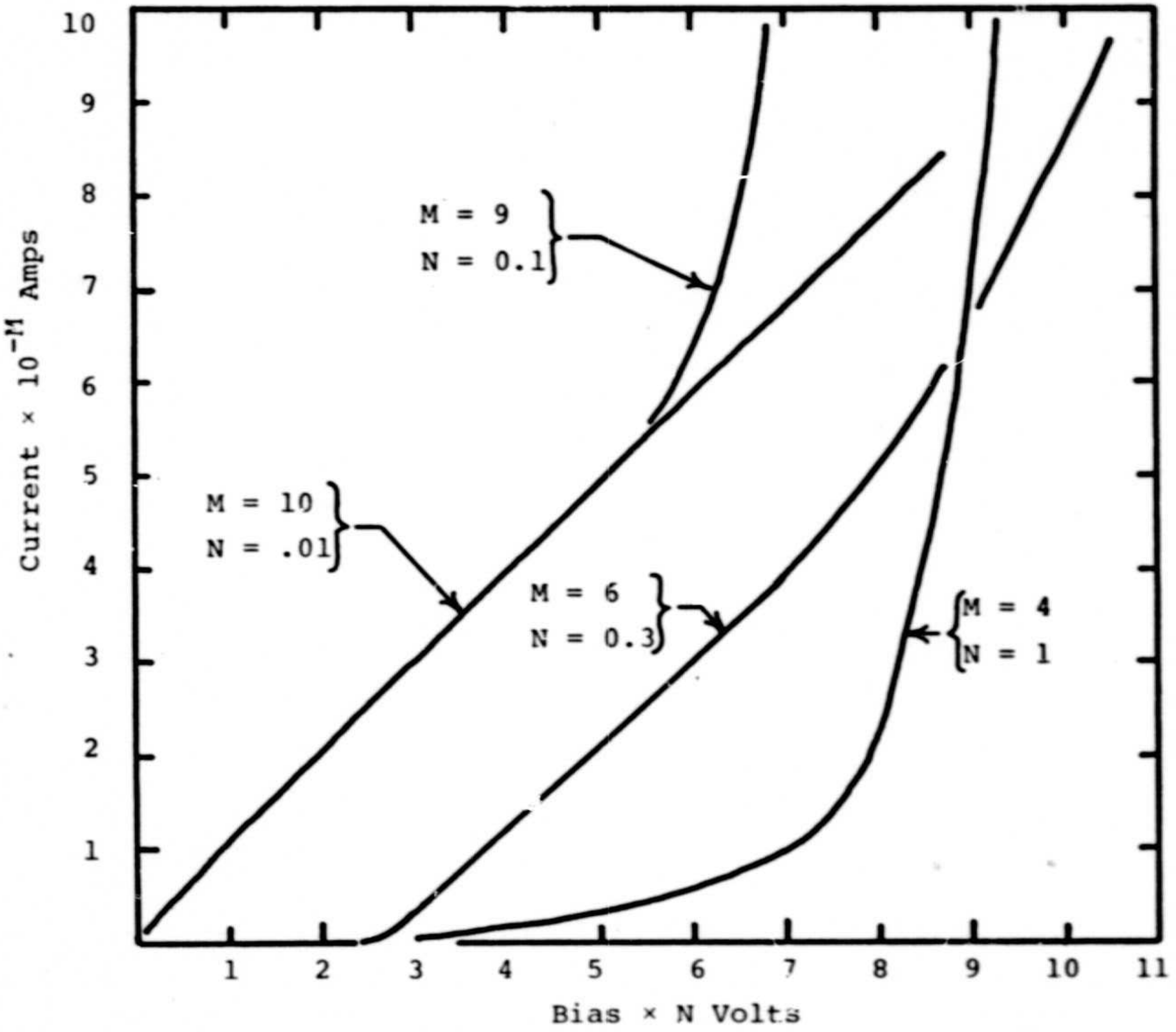

Figure 8

Forward I-V Characteristic at 77°K
of the same sample as is shown in Fig. 7.

the reverse resistance throughout the measurable range is $10^{10}\Omega$ at this temperature. The breakover to the second linear range occurs at 0.65 to 0.75 Volts at 77°K as opposed to 0.4 Volts at room temperature. The transition from the second linear region to superlinear behavior again occurs at approximately 2.5 Volts. This is followed by a second breakdown to a more superlinear behavior; this second transition is associated with the onset of visible light emission.

Electroluminescence

The heterojunction I-V characteristics results inspired an examination of the electroluminescence of ZnSe layers operated in this mode. Total visible electroluminescence data were taken using an EMI 9558-QB photomultiplier; this tube has an S-20 photocathode. This contrasts with the luminescence spectrum data which were taken using a tube with an S-10 photocathode and phase sensitive detection. In the present case both the sample and the detection apparatus was used in a D.C. mode and the photomultiplier tube was not cooled.

Samples were positioned on a cold finger in an evacuable chamber. Good thermal contact to the cold finger was not provided in general. The chamber was not evacuated for the room temperature measurements. The ZnSe surface was oriented to face the photocathode. Opaque contacts on the ZnSe obscured almost all of the nominal current carrying area. Only light emitted around the perimeter of the contact could therefore reach the photomultiplier. (Visual examination confirmed this expectation and showed that the illuminated zone width was comparable to the ZnSe thickness (20-50 microns). Lenses placed at the optical port of the sample chamber focused the emission on the photocathode; the equivalent aperture of this apparatus was approximately f/10.

Figure 9 shows the photomultiplier anode current versus forward bias voltage ($Au^{(+)}$-$Ge^{(-)}$) for a Zn vapor annealed ZnSe-HCl sample operated at liquid nitrogen temperature. A very sharp threshold for emission is evident at seven Volts; this threshold is reduced to approximately 5 volts at room temperature and the threshold becomes more diffuse. Figure 10 shows the photomultiplier anode current

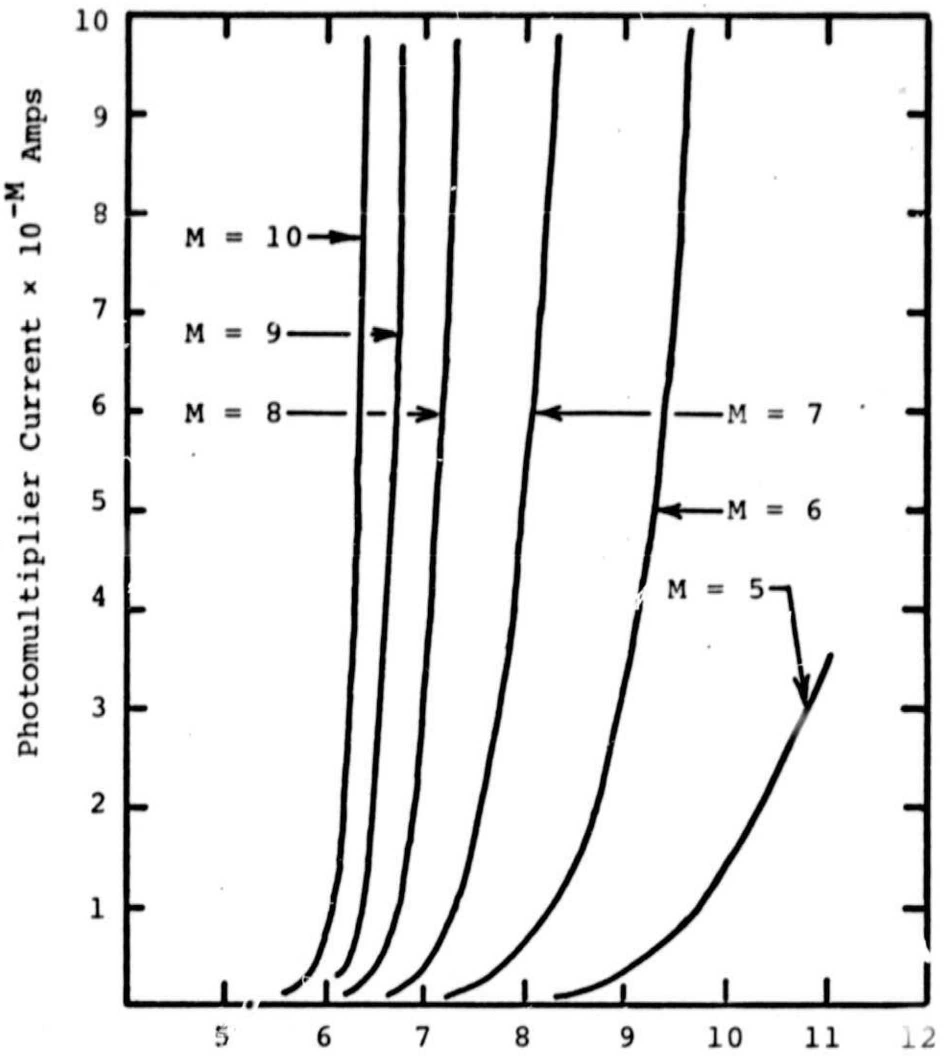

Figure 9

Electroluminescence at 77°K,
vs. Applied Voltage

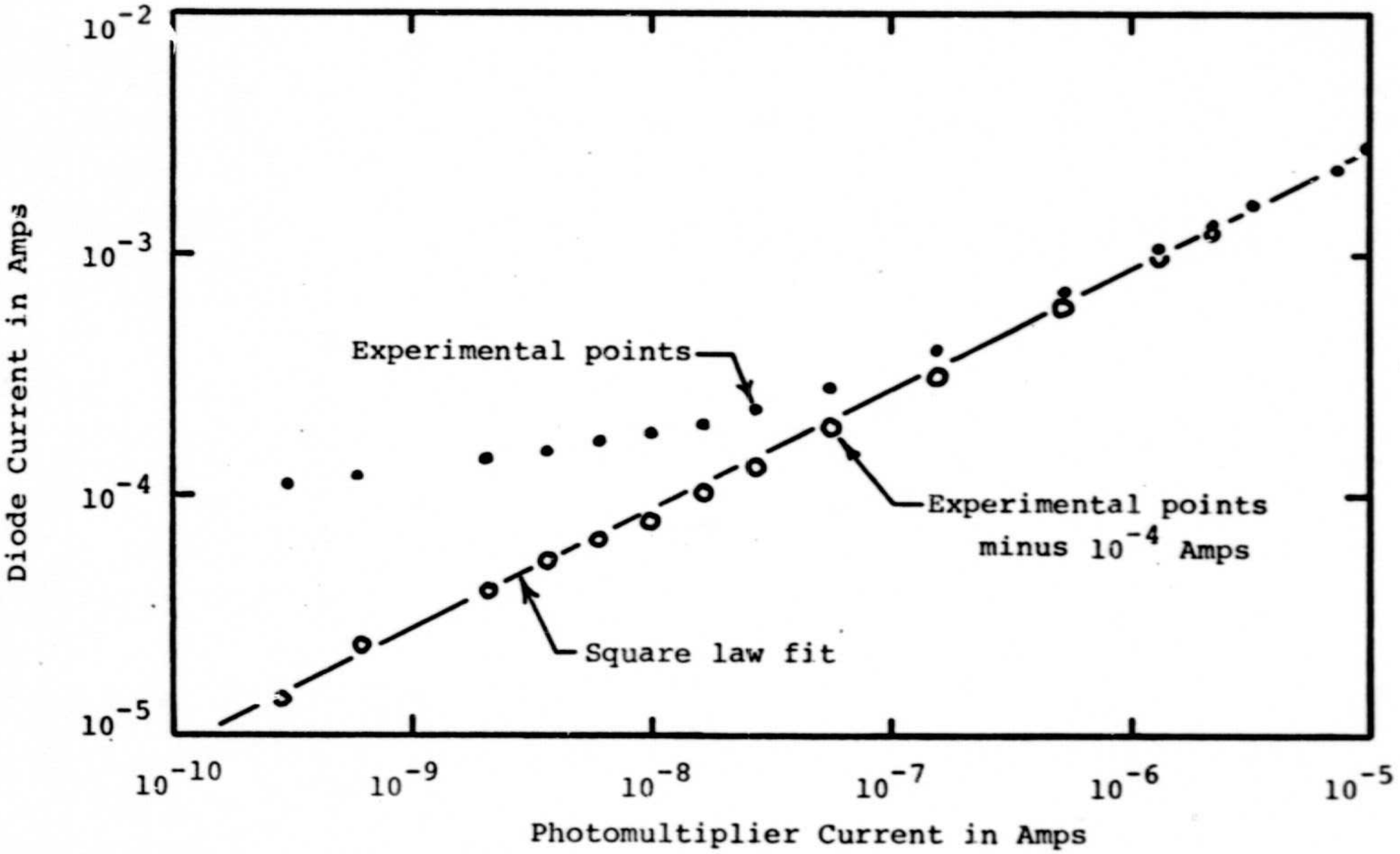

Figure 10

Electroluminescence at 77°K
vs. sample current.

versus forward bias current for the same sample at liquid nitrogen temperature. This data shows that the light emission is proportional to the square of the diode current. This quadratic relationship is also obtained at room temperature but the constant of proportionality is reduced by almost four orders of magnitude. The threshold current is only a factor of four higher at room temperature. The quadratic relationship is not understood although this relationship intuitively suggests a double injection mechanism. The threshold voltage is high enough that the holes required for luminescence could be generated by impact ionization. It is difficult to see how the electric field could be sufficiently concentrated near either the Au-ZnSe or ZnSe-Ge surfaces to lead to this process, however.

ZnSe layers grown in H_2 alone were annealed in Zn vapor and tested similarly for electroluminescence. The voltage threshold for electroluminescence at room temperature was the same as that for ZnSe-HCl samples even though these samples are approximately a factor of five thinner. No reliable luminescence data could be obtained from these samples at 77°K in general. This result is consistent with the very low forward bias currents that could be achieved at this temperature.

Intrinsic ZnSe layers annealed in an atmosphere of excess Se did not exhibit luminescence at either 77°K or 300°K. The same result was obtained from intrinsic ZnSe layers that were implanted with Na and subsequently annealed in Se. Na implanted layers annealed in Zn exhibited the same behavior as unimplanted layers.

It was not possible to search for electroluminescence in unannealed ZnSe-HCl layers since these samples would not pass appreciable current at room temperature. Unannealed and Zn annealed intrinsic ZnSe layers exhibited the same electroluminescence behavior at room temperature.

Electroluminescence Spectra

The electroluminescence spectra was taken using the same basic apparatus as was used for taking the U.V. stimulated luminescence data. The spectrometer is a one meter, double pass, grating unit with a blazing wavelength of 5500Å. A photomultiplier with an S-10 photocathode was used as the detector. The rapid rolloff in photocathode sentisivity in the range of 6000Å and longer wavelengths distorts the emission data in this region. In some cases the emission data were corrected for typical S-10 photocathode sensitivity and the spectral slit width of the monochromator. The actual system sensitivity versus wavelength was not determined. This partial correction brings the long wavelength data into agreement with published values of peak wavelength and linewidth for the well known lines. Electronic processing of the photomultiplier output is achieved by 13 hz phase sensitive detection. In normal operation an internal chopper modulates the emission and simultaneously generates an appropriately phased 13 hz square wave that is used as the reference signal. At low power levels a D.C. voltage was applied across the sample and the optical system was left as is. At high power levels the chopper was removed from the optical path so it generated the reference signal only. The reference signal was also processed using a PLL to generate a phase shifted 13 hz square wave. This shifted signal was used to gate a single polarity, current controlled pulse supply that excited the sample.

Samples were mounted in the same dewar assembly as was used for recording the U.V. stimulated fluorescence. The Ge sample substrates were soldered to brass blocks using In-Sn eutetic. These blocks were bolted to the cold finger. Vacuum deposited Au contacts were provided on the ZnSe surface and the ZnSe was glow discharged in H_2 prior to deposition in order to improve adhesion. Au wire spring leads were placed on the Au films to complete the electrical circuit.

Figure 11 compares electroluminescence and UV stimulated fluorescence at 77°K of 0.2% HCl samples. Electroluminescence was excited with a 16V square wave applied between a $2\times10^{-2}cm^2$ $Au^{(+)}$ contact and the Ge substrate. Both curves have been corrected for the response of the S-10 photocathode.

Figure 12 compares the electroluminescence spectra excited with 16V and 14V square waves. This figure is included to show the peak shift and linewidth change due to variations in excitation level. The shift of the peak to shorter wavelengths at higher excitation would normally exclude thermal effects and establish this as a donor-acceptor pair process. The ∿6000Å self-activated emission band has an anomolous thermal shift at temperatures below 250°K in that the peak wavelength decreases with increasing temperature.(5) Interrupted DC excitation was used to determine that thermal effects were present. The voltage was set at 10-12 Volts for these scans; this corresponds to lower average power than was used for the 14V and 16V pulse experiments. This DC voltage was interrupted and restarted at several points on the leading and trailing edges of the wavelength seen through the peak. Comparison of the emission intensity before and after interruption and the slopes of the intensity versus wavelength indicates that the major peak shift is due to a process with a time constant of several seconds. This must be a thermal process but a simultaneous donor-acceptor pair process cannot be excluded.

Figure 13 details the blue emission obtained by excitation with 16V and 14V square waves. The peak blue emission was compared with the peak yellow emission after correcting for the photocathode. The

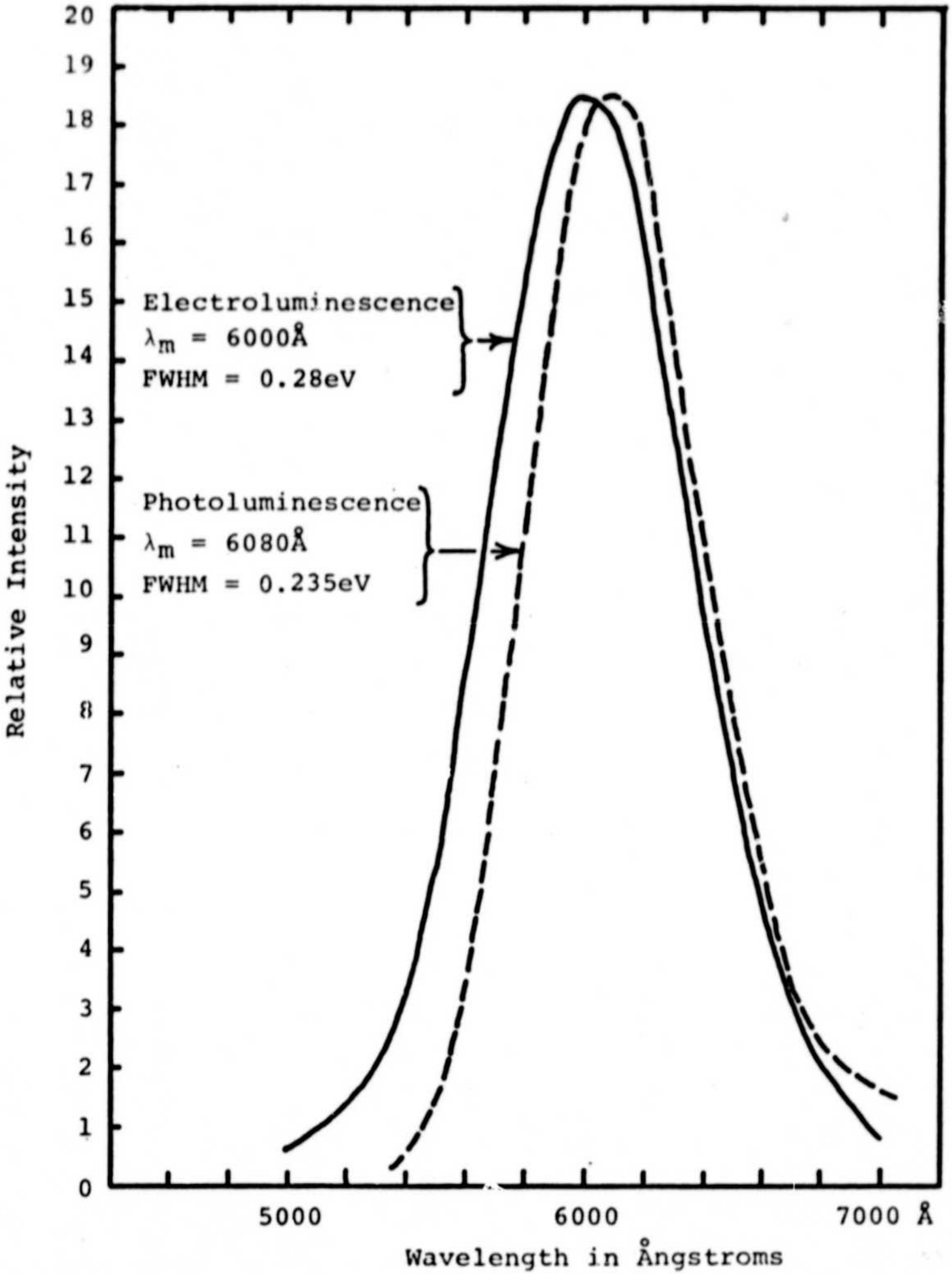

Figure 11

Comparison of Electroluminescence and Photoluminescence at 77°K

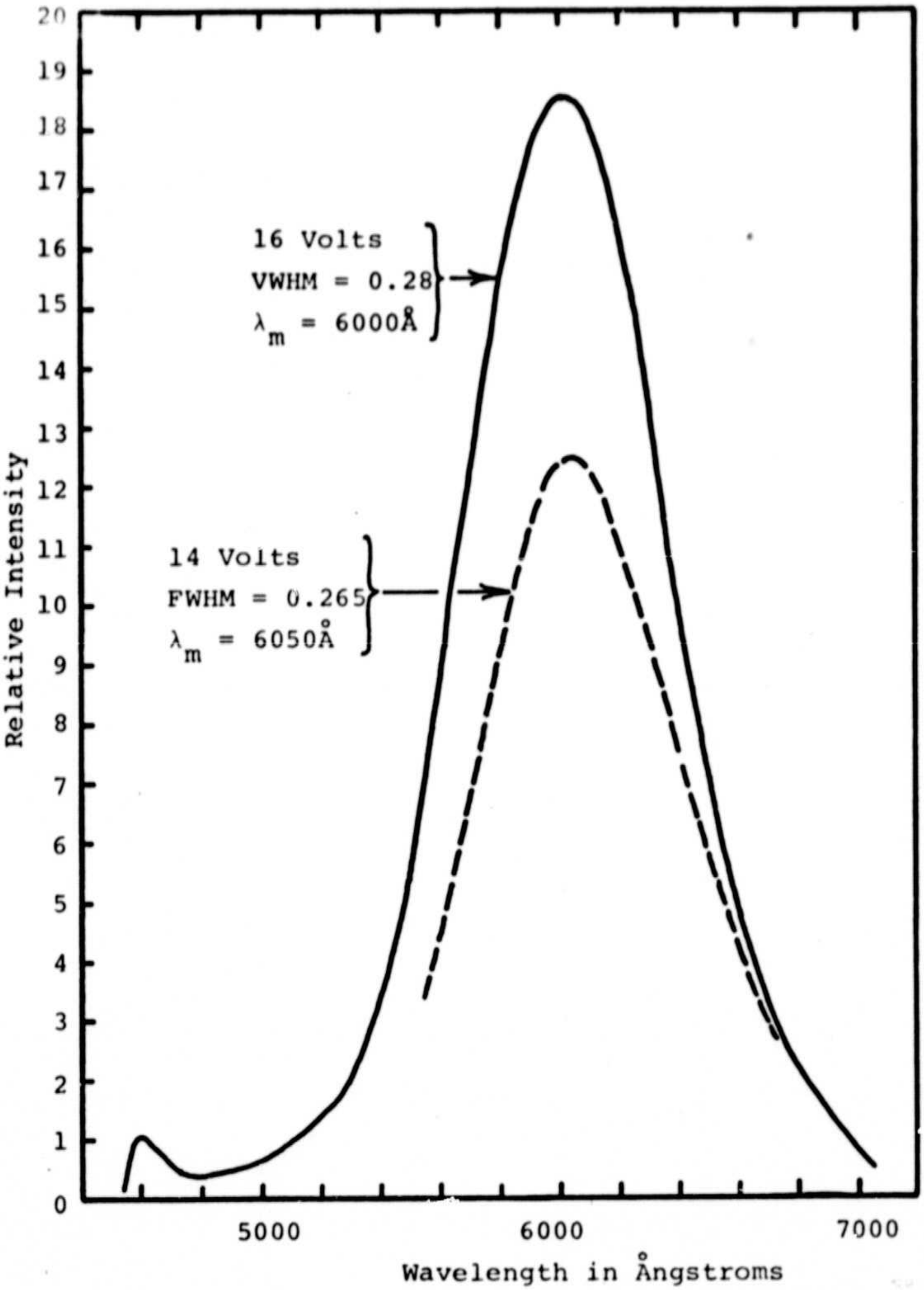

Figure 12

Electroluminescent Lineshape
vs. Excitation Amplitude

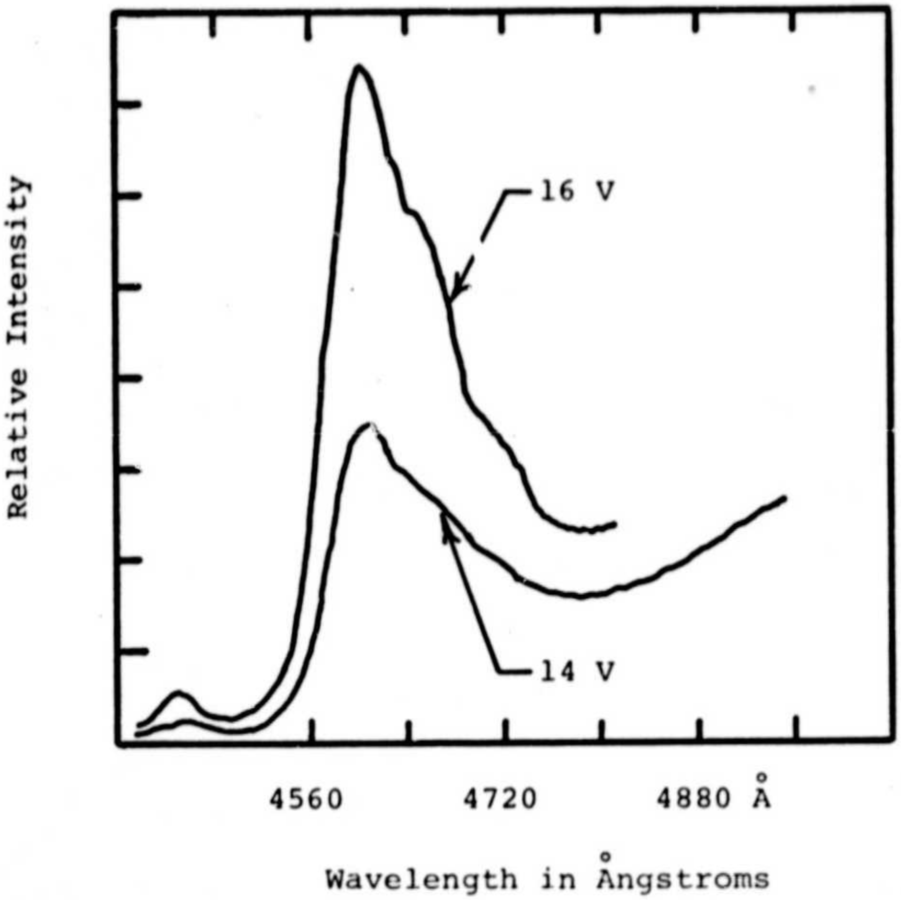

Figure 13

Blue Electroluminescence Detail

yellow/blue intensity ratio was 24/1 for the 14V scan and 19/1 for the 16V scan. This ratio was found to be 70/1 for 12V DC excitation of this sample. The change in this ratio with excitation intensity suggests saturation of the 6000Å transition. The broad, weak line observed between 4440Å and 4490Å in the data for 16V excitation is believed to be associated with the sharp 4450Å line observed under UV stimulation. The broadening may be due to Zn annealing, quench cooling induced strain, or the applied electric field.

Figure 14 shows the electroluminescence of an undoped (no HCl) sample using DC excitation at various voltages. This sample was annealed in Zn and then etched to leave a layer approximately 2 microns thick. The electroluminescence data in Figure 14 are drawn to a common aribtrary scale; the relative scaling of the photoluminescence data is arbitrary. The intensity of electroluminescence was extremely weak as is evidenced by the magnitude of the noise level, and graphical averaging was required in drawing these curves. The actual structure may be attenuated relative to that shown, but the similar features found in all the curves suggests that this averaging is not completely dishonest. The shift in the emission spectra to shorter wavelengths at higher excitation levels is quite definite; little else can be said about the spectra since the features and their origin are not understood. The primary experimental difficulty with this sample originated with an excessive thickness reduction during etching. The resulting layer suffered permanent electrical breakdown at just over 14 Volts.

Figure 15 shows the electroluminescence spectra of HCl grown, Zn annealed samples at room temperature; the spectra has been corrected for photocathode response. This sample was provided with a $2x10^{-2}cm^2$ opaque Au front contact. The data were taken while driving the sample

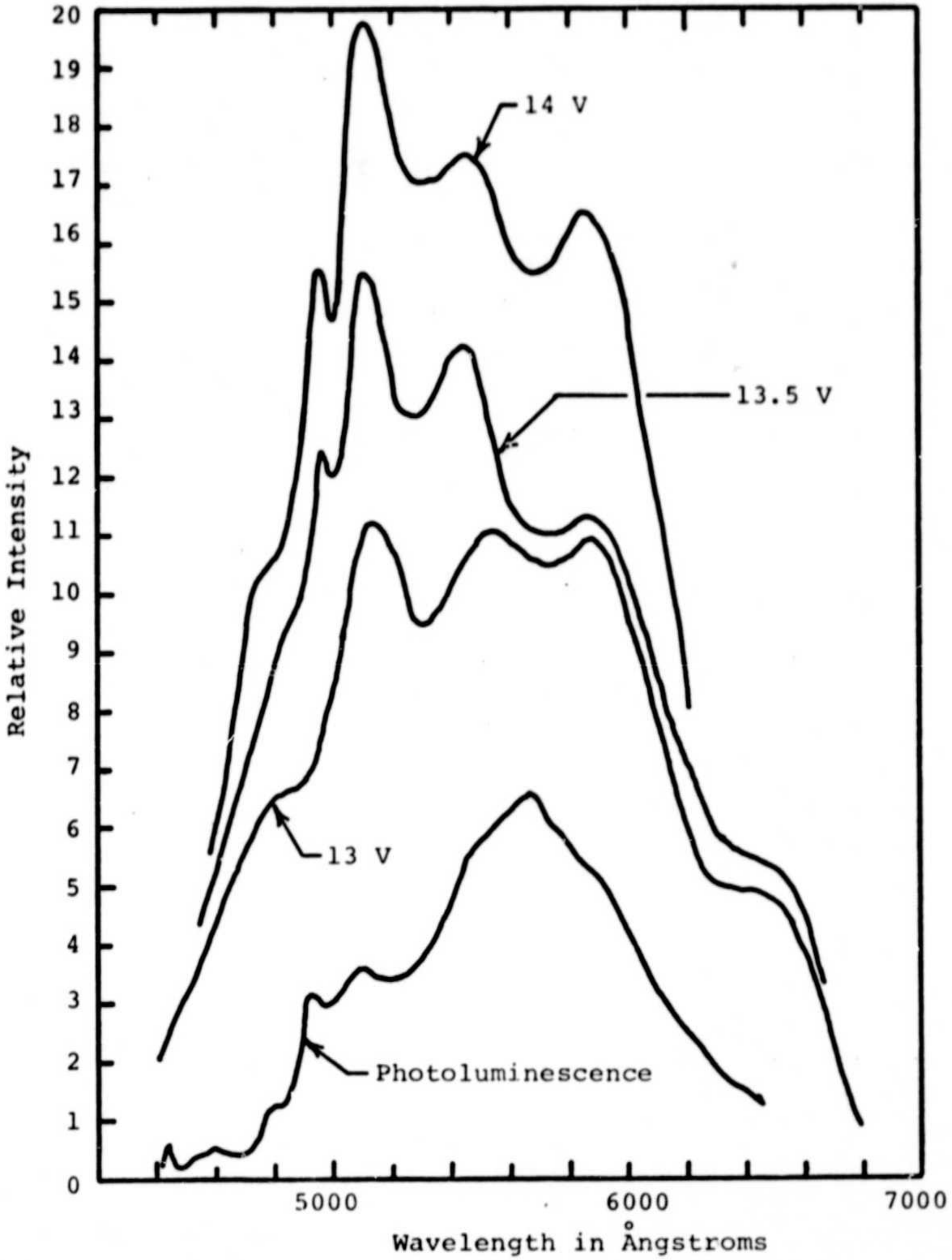

Figure 14

Electro- & Photo-luminescence at 77°K of ZnSe samples grown in H_2 only.

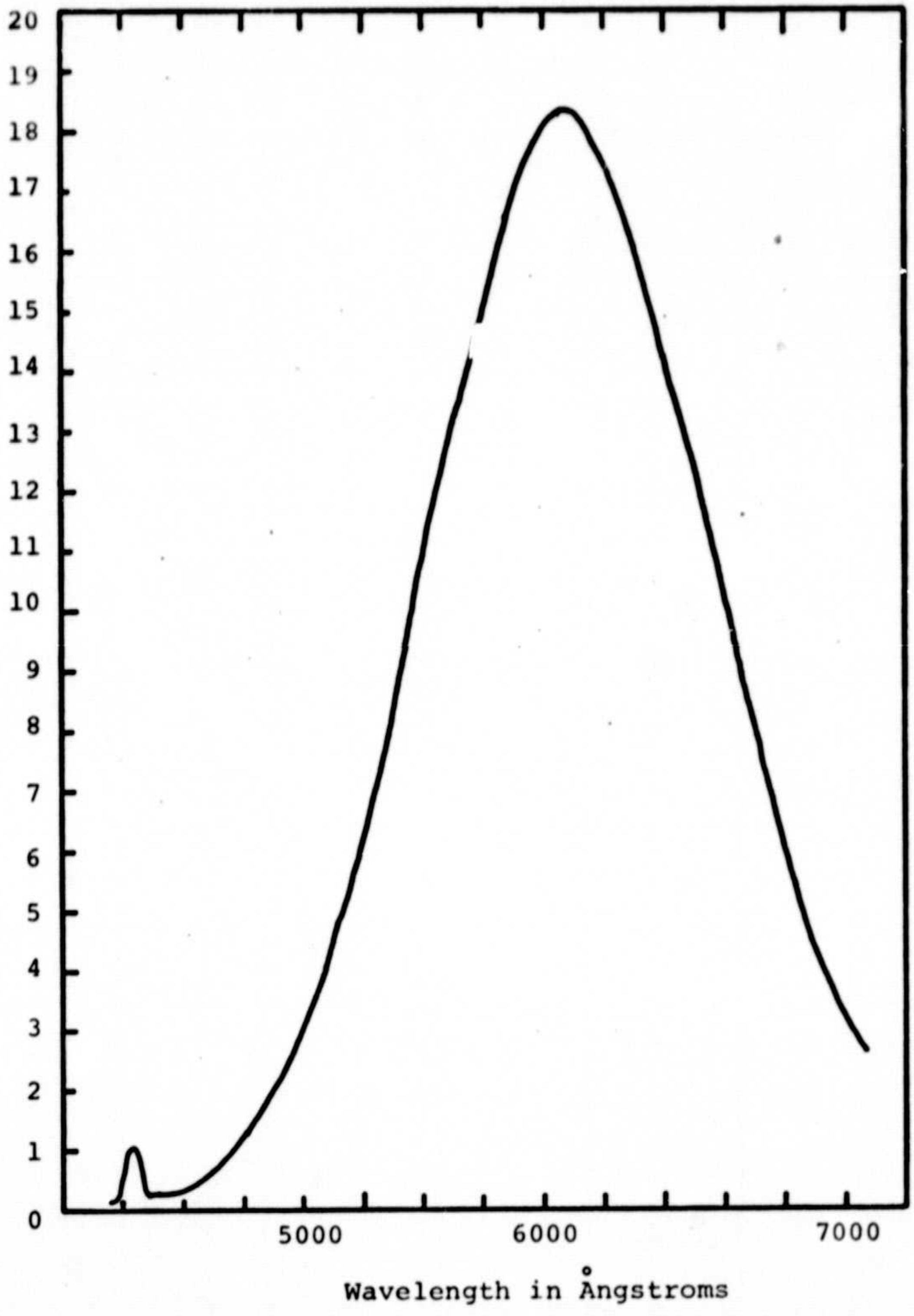

Figure 15

Electroluminescence at 300°K

with a 25V, 13 hz square wave. The sample current of 110 mA implies an average power of $\sim$1.4 Watts. Visual examination reveals a narrow orange-yellow halo around the contact perimeter. This halo is readily visible in room light and becomes noticeably more yellow at higher excitation voltages.

Only a few H_2 grown ZnSe layers were examined for electroluminescence at room temperature. In some cases this luminescence appeared to be a faint green. In most cases the luminescence appeared to be a faint white; it is believed that the white appearance is due to the intensity being lower than the color sensitivity of the eye. In a few cases relatively bright yellow and/or green points were observed on the perimeter of the ZnSe contact. Each of these points emitted for a few minutes at most and there was a change in the I-V characteristic as each point extinguished. A room temperature spectra was not obtained for ZnSe-H_2 grown layers.

Implantation

H_2 grown ZnSe layers were implanted with ^{23}Na at room temperature.(16,17) Implants were performed normal to the surface, or equivalently along the (100) direction. The samples were implanted at 80 keV to a dose of $3\times10^{14}/cm^2$ followed by a 20 keV implant to a dose of $1\times10^{14}/cm^2$. If it is assumed the implanted ions achieve only the amorphous target range, this implies a reasonably uniform Na doping to a depth of ∿1500Å with a surface concentration of $\sim10^{20}/cm^3$ and a concentration of $10^{19}/cm^3$ at 1500Å.(18) Channeling could increase these ranges by a factor of three and reduce the concentrations by a factor of three; the magnitude of possible Na diffusion effects is impossible to estimate a-priori. A reference sample was implanted in the same manner but with the dose reduced by a factor of ten. The implantations were performed through Ta contact masks; the masks were machined to yield an implanted area in the form of a Van der Pauw clover-leaf.

None of the as-implanted samples exhibited any visible photoluminescence at either 300°K or 77°K. The photoluminescence of the unimplanted area was not affected by these processing steps. Thermal probe measurements of the as-implanted samples were either ambiguous or indicated that the layer remained n-type. Van der Pauw resistivity measurements of the as-implanted samples indicates resistivities of $\sim10^{9}\Omega/\square$. Vacuum deposited Au contacts were employed for these measurements. (The resistivity of unimplanted samples was greater than $10^{12}\Omega/\square$.)

One implanted sample was examined for crystallinity using high energy electron diffraction. This apparatus employs a 40 keV glancing electron beam to interrogate the lattice structure to a depth of 50Å.

ORIGINAL PAGE IS
OF POOR QUALITY

This HEED system is ion pumped and maintained at a pressure of 10^{-10} Torr. Spot patterns were not observed initially from either the implanted ZnSe, the unimplanted ZnSe, or the Ge substrate. One-half hour, isochronal anneals were then performed in situ in increments of ∿100°C.

The 100°C anneal led to no effect. Orange cathodoluminescence was visible on the unimplanted ZnSe after the 200°C anneal and there was very faint green luminescence in the implanted area; there was still no spot pattern from any part of the sample. 300°C annealing led to a good diffraction pattern from the germanium substrate and a dubious pattern from the unimplanted ZnSe; the cathodoluminescence intensity increased but there was no diffraction pattern from the implanted ZnSe. Subsequent temperatures up to 600°C did not lead to any changes except for an improvement in the clarity of the behavior already observed. At a temperature of 650°C the ZnSe layer became detached from the Ge substrate. It can be concluded that the ZnSe surface becomes amorphous as a result of the $4\times10^{14}/cm^2$ implant and that crystallinity cannot be restored by annealing in vacuum. The appearance of a spot pattern after 300°C annealing can be associated with desorption of surface contaminants.

Samples were also annealed isochronally for one-half hour periods in a Se atmosphere and then quench cooled. These anneals were performed in evacuated and sealed ampoules. The ampoules were placed in a two zone furnace where an excess Se pressure was provided by maintaining a Se pellet at 200°C while the ZnSe temperature was adjusted between 200°C and 600°C. This annealing did not lead to visible photoluminescence for any of the above annealing conditions. No evidence of p-type thermal probe signals were obtained. (Au contacts provided for electrical measurements were not affected by subsequent Se anneals.) Van der Pauw measurements indicated that the resistivity increased to values higher than those obtained in unimplanted samples. Van der Pauw mobility measurements were impossible due to the impedance levels. It is still possible that a shallow surface layer was converted p-type and that the sheet resistivity increased as a result of junction isolation and the thinness of the conducting layer.

Capacitance measurements of these annealed layers show the formation of a two to three micron thick intrinsic layer. Attempts to apply bias between the ZnSe and the Ge yielded I-V characteristics similar to back to back diodes; there was no measurable electroluminescence.

Na implanted samples were also annealed in Zn atmospheres. Photoluminescence was not recovered as a result of annealing up to the maximum temperature of 575°C. The electrical properties of Na implanted, Zn annealed samples could not be distinguished from those of unimplanted, Zn annealed samples.

Na implantations were chosen initially on the basis of the photoluminescence results of Chatterjee et al. and the expectation that group I impurities substituting for Zn should lead to shallower acceptors.(16,17,19) This study could not be completed, and it may still be possible to achieve type conversion by Na implantation. It may be that the ZnSe recrystallization temperature lies at temperatures above those where the ZnSe film detaches from the Ge substrate. Implanted Na should behave in a manner similar to that of implanted Li and yield a shallower acceptor level.(20) Successful studies with implanted Li suggest that ∿400°C anneals should be sufficient.(21) On the other hand, activation of implanted Al requires annealing at a temperature of 900°C.(22)

Growth of Undoped ZnSe on Cl Doped ZnSe

Only two attempts were made to grow ZnSe layers in H_2 on ZnSe layers grown in HCl. Ge substrates were prepared in the normal fashion and ZnSe layers were grown in 0.2% HCl for ~2 hours. This yields a ten micron Cl doped ZnSe layer. At the end of the nominal HCl growth period, the HCl flow was terminated but the H_2 flow and power to the heaters was maintained. This results in the normal conditions for H_2 growth; the continuing H_2 flow should purge the growth tube of HCl in approximately 10 minutes. The system was left in this state for 10 hours before terminating the growth entirely. In one case the system was intentionally jarred 30 minutes after turning off the HCl; this procedure displaces the substrate slightly and should yield a visible step on the epitaxial layer if growth continues after turning off the HCl.

There was no clear evidence of continued ZnSe growth in either case. The growth step on the sample that had been jarred could not be found, but this may be due to a poorly defined edge resulting from a poor contact between the sample and the crown after displacement. There appears to be a slight change in morphography after H_2 growth, but this is inconclusive. The morphography is quite similar to that of HCl grown ZnSe. Finally UV stimulated fluroescence studies show spectra very similar to HCl grown layers and the differences are not characteristic of H_2 grown layers. It must be concluded that either no growth occurred, or that the growth was so slight that the UV excitation penetrated to the HCl grown layer, or that Cl diffused into the H_2 grown layer from the previous layer. Hovel and Milnes report that they were not able to obtain ZnSe gorwth on ZnSe under identical conditions without either a halogen or exposed Ge present to act as a chemical transport agent.(1) It may be necessary to introduce Ge by some mechanism in order to obtain the desired growth. This does not introduce a new parameter since all the previous luminescence data on H_2 grown ZnSe refers to growth in the presence of Ge. Annealing and electroluminescence studies were not performed on these hypothetically compound structures.

Conclusions

Undoped, epitaxial ZnSe layers can be grown on (100) Ge using the close-spaced transport process. These layers are grown at the relatively low substrate temperature of 575°C using a ZnSe source temperature of 675°C. Growth is achieved in a flowing H_2 atmosphere; interaction of ZnSe and the Ge, presumably in the form of $GeSe_x$, and the Ge acts as a chemical transport agent. The role of the Ge in the growth process explains the virtual termination of ZnSe growth at a layer thickness of approximately ten microns. A determination of the Ge contamination of the ZnSe layers should be performed.

These ZnSe layers exhibit UV stimulated fluorescence superior to that of source ZnSe and comparable to the best, bulk ZnSe data appearing in the literature. Superior, in this instance, refers to the relative intensities of near bandgap as opposed to low energy emission and the structured detail of the near bandgap emission. Although some ZnSe purification occurs in the growth process, there is enough variability in the spectra of the layers to indicate that prepurification of the ZnSe sources should be attempted in order to obtain reproducible results.

Annealing these samples in Zn vapor leads to limited n-type conductivity and degradation of the fluorescence efficiency. This result refers to annealing in a single zone furnace at 575°C where the Zn vapor pressure and the sample annealing temperature are functionally related. Formation of a Zn-Ge compound and destruction of the sample can occur in this configuration. The relationship between annealing, conductivity, and fluorescence efficiency should be investigated using a two zone furnace where the lower temperature zone is used to independently control the Zn vapor pressure.

The ZnSe layers do not exhibit any adhesion problems. Cracking, which might be expected due to the difference in the thermal expansion coefficients of Ge and ZnSe, does not appear after the relatively rapid cool down after growth or after quenching after annealing.

There is no evidence to indicate that ZnSe epitaxial layers can be grown on ZnSe using the process (source T=675°C, substrate T=575°C, and H_2 gas only). Additional experimentation would be required to answer this question; it may be necessary to place Ge in growth region to obtain epitaxial layers.

There is also no evidence to indicate that Na implantation can be used to type convert these layers. Isochronal anneals at temperatures up to 575°C and in both Se and Zn atmospheres lead to inconclusive results. The annealing temperatures required for recrystallization of implanted ZnSe is not established and the adhesion of the ZnSe epitaxial layer at this temperature is an open question.

Thick, epitaxial ZnSe layers can be grown on (100) Ge using the close-spaced, chemical transport process. Growth is achieved in a flowing H_2 atmosphere with a small percentage of HCl added and at a substrate temperature of 575°C and a source temperature of 675°C. The growth rate increases with increasing HCl concentration and becomes polycrystalline at an HCl concentration of 0.6%. Macroscopic variations in growth rate and morphography appear at HCl concentrations below 0.1%. An HCl concentration of 0.2% yields a growth rate of 5 microns/hour and leads to the best compromise between uniformity and growth rate.

The UV stimulated fluorescence spectra of these ZnSe layers is typical of Cl doped, bulk ZnSe. The dominant orange emission is reproducible and increases in intensity with increasing HCl concentration. The emission in the 4400 to 4700 Å range reduces with increasing HCl concentration.

Annealing the layers at 575°C in a Zn vapor atmosphere followed by quench cooling to room temperature yields n-type conductivity. Quench cooling is required to maintain this conductivity. Quench cooling 50 micron thick films leads to (100) oriented cracks in the epitaxial layer; the layers must be etched to make these cracks visible. Etching as-grown layers, however, does not show any cracking problem associated with the relatively rapid cool-down (∿15 min.) after growth. The induced conductivity is linearly related to the Zn vapor pressure during annealing. The Zn reservoir temperature must be lower than the sample temperature during annealing to prevent excessive Zn attack of the Ge substrate. This limits the Zn vapor pressure. The maximum Zn temperature of 525°C (P_{Zn} = 3 Torr) leads to a resistivity of $\sim 10^3$ Ω-cm which is too high for the intended application. Annealing in Zn vapor at higher sample temperatures could be investigated, but annealing in vacuum leads to adhesion failure at 650°C.

Zn doping of the Ge substrate occurs both during growth and subsequent Zn vapor annealing. This effect is established by measurements showing formation of a p-type layer on the Ge in the growth area. This process and possible Ge migration into the ZnSe may contribute to the limited ZnSe conductivity achieved by Zn vapor annealing. Reverse bias on the ZnSe-Ge heterojunction ($ZnSe^{(+)}-Ge^{(-)}$) leads to electron injection into the ZnSe; this must be due to tunneling between the Ge valence band and the ZnSe conduction band.

Zn vapor annealed, 0.2% HCl ZnSe layers that are provided with

Au contacts on the ZnSe exhibit bright yellow-orange electroluminescence at room temperature. The samples are operated as heterojunctions with the Au contact biased positively and the Ge substrates biased negatively. The threshold for detectable emission occurs at 5-6 Volts and the emission is readily visible at 10-12 Volts.

This electroluminescence device may be of some value in its present configuration. Some modifications should make the device more efficient. The Ge substrate should be made conducting p-type by either Al or Ge doping. This would eliminate a series resistance problem. This doping plus any transfer of the dopant to the ZnSe would make the ZnSe at the interface more n-type and would also enhance tunneling by reducing the tunneling barrier. If it is assumed that the tunneling in the present case is actually to the ZnSe conduction band and not to a Cl impurity band and if transfer of the dopant does occur, it would be possible to obtain a similar electroluminescent device using undoped (no HCl) ZnSe layers. Al or Ga doping near the ZnSe-Ge interface would permit electron injection and simultaneously provide a barrier preventing holes from escaping to the Ge. The wavelength of emission of this device should be shorter than that of the 0.2% HCl grown device. This new approach avoids the problems of cracking during quench cooling that occurs in the thicker layers grown in HCl and the problems of growing undoped ZnSe on doped ZnSe. As a result, ion implantation to obtain type conversion and higher hole injection efficiency could be pursued without first solving these problems. The concept of employing double injection into an undoped, high optical quality layer is retained.

References

1.) Hovel, H.J. and A.G. Milnes, J. Electrochem. Soc. 116, 843 (1969).

2.) Nicoll, F.H., J. Electrochem. Soc. 110, 1165 (1963).

3.) DiLorenzo, J.V., J. Electrochem. Soc. 118, 1645 (1971).

4.) Stringfellow, G.B. and R.H. Bube, Phys. Rev. 171, 903 (1968).

5.) Jones, G. and J. Woods, J. Phys. D. Appl. Phys. 9, 389 (1974).

6.) Dean, P.J. and J.L. Merz, Phys. Rev. 178, 1310 (1969).

7.) Espinosa, G.P., T.C. Lim, E.S. Cory, R. Zucca and Hengstenberg, Appl. Phys. Letters 26, 514 (1975).

8.) Gebhardt, E., Z. Metallkunde 34, 255 (1942).

9.) Parker, S.G., J. Crystal Growth 9, 177 (1971).

10.) Park, Y.S., C.R. Geesner and B.K. Shin, Appl. Phys. Letters 21, 567 (1972).

11.) Sze, S.M., Physics of Semiconductor Devices, Wiley, 1969, p. 31.

12.) Milnes, A.G. and D.L. Feucht, Heterojunctions and Metal-Semiconductor Junctions, Academic Press, 1972, p. 65.

13.) Hovel, H.J. and A.G. Milnes, Int. J. Electron. 25, 201 (1968).

14.) Hovel, H.J. and A.G. Milnes, IEEE ED-16, 766 (1969).

15.) Milnes, A.G. and D.L. Feucht, Heterojunctions and Metal-Semiconductor Junctions, Academic Press, 1972, p. 163.

16.) Ibuki, S., H. Komiyz, A. Milsuishi, A. Manaloc and H. Yoshirya, II-VI Semiconducting Compounds, ed. D.G. Thomas, Benjamin, 1967, p. 1140.

17.) Tell, B., J. Appl. Phys. 42, 2919 (1971).

18.) Gibbons, J.F., W.S. Johnson and S.W. Mylroie, Projected Range Statistics, Dowden, Hutchinson & Ross, Stroudsburg, Penn., 1975.

19.) Chatterjee, P.K., A.J. Rosz, and B. G. Streetman, J. of Luminescence 8, 176 (1973).

20.) Dieleman, J., J.W. DeJong and T. Meijer, J. Chem. Phys. 45, 3178 (1966).

21.) Park, Y.S. and C.H. Chung, Appl. Phys. Lett. 18, 99 (1971).

22.) Shin, B.K., Y.S. Park and D.C. Loole, Appl. Phys. Lett. 24, 435 (1974).